Quantitative Analysis of Anterior Chamber Inflammation Using the Novel CASIA2 Optical Coherence Tomography

MINGZHI LU, XIAORAN WANG, LEI LEI, YANG DENG, TINGLONG YANG, YE DAI, YONGHAO LI, XIAOLIANG GAN, YIXIN HU, HUI CHEN, MENG LI, LISHI SU, JIN YUAN, AND WEI CHI

• PURPOSE: We evaluated the clinical utility of a novel anterior segment optical coherence tomography (AS-OCT) device, CASIA2, to evaluate parameters indicative of anterior chamber (AC) inflammation severity in uveitis, including AC cell number, flare, and keratic precipitates (KPs).

• DESIGN: Prospective evaluation of a diagnostic device.

• METHODS: Uveitis eyes were classified into active and inactive groups. The number of hyperreflective dots representing AC cells and optical density ratio (aqueous-to-air relative intensity [ARI] index) for flare qualification were calculated from AS-OCT images. In addition, a program was designed to quantify the posterior corneal surface smoothness (PCSS) of each image for KPs evaluation. The maximum, minimum, and average PCSS values were calculated from 128 images per eye and compared among active uveitis, inactive uveitis, and control eyes. Correlations between Standardization of Uveitis Nomenclature grade and both hyperreflective dot number and ARI index were evaluated. Receiver operating characteristic (ROC) curves were constructed to test the values of these indicators for uveitis diagnosis.

• RESULTS: AC hyperreflective dot count, ARI index, and maximum and average PCSS values were all significantly higher in the active uveitis group than in the inactive and control groups. Hyperreflective dot count and ARI index were associated with Standardization of Uveitis Nomenclature cell and flare grade. According to ROC curve analysis, maximum PCSS was the best indicator for the diagnosis of uveitis involving the anterior segment, meanwhile the hyperreflective dot number was the best to identify active AC inflammation from the inactive.

• CONCLUSIONS: Quantification of AC cell number, flare, and KPs using the CASIA2 device is a promising strategy for the objective assessment of AC inflammation. (Am J Ophthalmol 2020;216:59–68. © 2020 Elsevier Inc. All rights reserved.)

UVEITIS IS ONE OF THE MOST COMMON CAUSES OF blindness worldwide.[1–5] The precise evaluation of intraocular inflammation in uveitis is necessary for diagnosis, classification of disease severity, and estimation of intraocular activity. Moreover, timely and accurate severity grading of intraocular inflammation is vital for choosing the appropriate therapeutic measures. At present, the standard clinical approach for anterior chamber (AC) inflammation grading is Standardization of Uveitis Nomenclature (SUN) scoring from slit-lamp images.[6] However, SUN score is highly subjective, leading to marked differences across evaluations. Moreover, the individual variance in the reported number of AC cells, a cardinal feature of uveitis, can be exacerbated by certain test conditions, such as the brightness of the slit-lamp light strip.[7] Advances in optical imaging technology offer new opportunities for objective, accurate, and quantitative assessment of AC inflammation. Laser flare-cell photometry, a fast and noninvasive technique, is mainly used to quantify AC flare and cell number by measuring the amount of light scatter from AC particles.[8,9] However, laser flare-cell photometers are expensive and there is still no consensus on their clinical utility.[10] Moreover, the accuracy of the instrument for cell counting is lower than for quantifying flare.[11] These problems have limited the widespread application of laser flare-cell photometry in clinical practice.

Recently, high-resolution anterior segment optical coherence tomography (AS-OCT) was introduced for the evaluation of AC inflammation.[12–19] Commercial AS-OCT devices feature a variety of axial and transverse resolutions. The newer CASIA2 model (Tomey, Nagoya, Japan) is a swept-source spectral-domain OCT device that uses a longer wavelength (1310 nm) to image the entire AC in 128 cross-sectional images spaced 1.4° apart. The instrument also has improved scanning speed and scanning density to ensure high-resolution imaging of the AC. Several studies have used CASIA2 to assess cataract, glaucoma, and other ocular surface–related conditions.[20–26] However, there is no report evaluating the utility of CASIA2 for observing the AC inflammation of uveitis.

AJO.com Supplemental Material available at AJO.com.

Accepted for publication Mar 18, 2020.

From the State Key Laboratory of Ophthalmology (M.L., X.W., L.L., Y.D., Y.D., Y.L., X.G., Y.H., H.C., M.L., L.S., J.Y., W.C.), Zhongshan Ophthalmic Center, and the School of Public Health (T.Y.), Sun Yat-sen University, Guangzhou, China.

Inquiries to Wei Chi, State Key Laboratory of Ophthalmology, Zhongshan Ophthalmic Center, Sun Yat-sen University, 54 Xianlie Road, Guangzhou 510060, China; e-mail: chiwei@mail.sysu.edu.cn

0002-9394/$36.00
https://doi.org/10.1016/j.ajo.2020.03.032

Given the advanced functions of this novel AS-OCT system, we examined the feasibility of using CASIA2 to objectively quantify and grade AC inflammation in patients with uveitis involving the AS.

In the present study, we used the CASIA2 device to quantify the 3 important signs of uveitis involving the AS, keratic precipitates (KPs), number of AC cells, and aqueous flare, and our findings showed that those parameters measured by computational analysis of CASIA2 images could take the place of traditional subjective assessment using slit lamps to objectively and quantitatively evaluate the anterior inflammation in uveitis.

METHODS

• **PARTICIPANT SELECTION AND CLINICAL EXAMINATION:** This study was approved by the Ethics Committee of the Zhongshan Ophthalmic Center, Sun Yat-sen University of China (2019KYPJ106) and adhered to the tenets of the Declaration of Helsinki. Ninety-one eyes of 62 patients examined at Zhongshan Ophthalmic Center from May 2018 to February 2019 were enrolled in this study. All patients were diagnosed with unilateral or bilateral uveitis involving the AS (56 eyes with active inflammation and 35 eyes with inactive inflammation). During the same period, 48 eyes of 24 healthy volunteers without a history of ocular inflammation, injury, surgery, or other remarkable ocular diseases were recruited. Eyes were excluded because of keratopathy, such as corneal opacity, corneal edema, corneal guttata, or scar. All participants received a comprehensive ocular examination conducted by uveitis specialists (W.C., Y.D.), including best-corrected visual acuity (BCVA) and intraocular pressure measurements, slit lamp biomicroscopy of the AS, and binocular indirect ophthalmoscopy of the posterior segment. AC inflammation was graded from 0-4 according to the SUN criteria. The number of AC cells was counted in a standard field defined by a 1 × 1 mm slit beam centered on the center of the cornea. The grading scale was 0 for no detected cells, 0.5+ for 1-5 cells per field, 1+ for 6-15 cells, 2+ for 16-25 cells, 3+ for 26-50 cells, and 4+ for >51 cells.[6] Patients with uveitis involving the AS were classified into the active or inactive group based on the clinical AC inflammation grading scale (0 for inactive, 1-4 for active). Informed consent was obtained from all participants at enrollment.

• **CASIA2 IMAGE ACQUISITION:** All uveitis eyes and control eyes were imaged using the CASIA2 by a trained operator blinded to the precedent diagnostic results. This swept-source OCT device can image the cornea and anterior part of the eye at 50,000 A-scans per second using a swept-source light of 1310 nm. The configurational specifications stated by the manufacturer include axial resolution of 10 μm, lateral resolution of 30 μm, minimal lateral scan dimension of 16 mm, and maximal scan depth in tissue (axial direction) of 13 mm. In a darkened room, each patient was requested to keep staring at 1 fixed internal point during the entire scanning process. To prevent frequent blinking, manual support was applied to the eyelids with minimal pressure affecting the bulb. The quality of A-scan images was assessed during acquisition by the operator. One hundred twenty-eight cross-sectional images were recorded for each eye, and the selection of images for further analyses was determined by the specific aim of each study section.

• **IMAGE ANALYSIS:** The same trained operator who was blinded to previous diagnosis counted the number of hyperreflective distinct dots for estimating AC cell count using Image J software (https://imagej.net). Briefly, the technician used the polygon selection tool to select the entire AC area. To reduce noise interference, image processing was performed with binarization. Starting from the horizontal position (0°-180°), 8 evenly distributed OCT images (every 22.5°) were obtained for each eye. The dot counts of the 8 cross-sectional images of each eye were averaged as the final result (Figure 1).

Analysis of aqueous flare was based on the method of Invernizzi and associates.[17] Adobe Photoshop CS6 software (Adobe Inc., San Jose, California, USA) was used to obtain an average brightness value for 200 × 200 pixels in the AC area below the apex of the cornea (aqueous intensity). The same method was used to obtain the average brightness value of a smaller area (100 × 100 pixels) in the upper right corner outside the eye (air intensity). Aqueous-to-air relative intensity (ARI) index was defined as ratio of the luminance value in the AC to that of air. The ARI index values were multiplied by 100 for convenience in statistical calculations. Intensity measurements of the 8 cross-sectional images per eye were averaged as the final result (Figure 2, E and F).

An algorithm for quantifying the smoothness of the posterior corneal surface as a measured of KP number was developed for Matlab R2019a (https://ww2.mathworks.cn). Briefly, the boundary between the posterior surface of the cornea and the AC was identified and the tangent angle of each point was automatically calculated through the boundary. The standard deviation of all tangent angles was counted as the final output value. The final output value was defined as posterior corneal surface smoothness (PCSS). A PCSS value near 0 indicates maximum smoothness of the posterior cornea surface, while a value near 1 indicates maximum roughness. The maximum (MAX), minimum (MIN), and average (AVG) PCSS values of all 128 sections per eye were automatically calculated by the software (Figure 2, A through D).

• **STATISTICAL ANALYSIS:** GraphPad Prism 8.0 software (GraphPad Software, Inc., La Jolla, California, USA) was

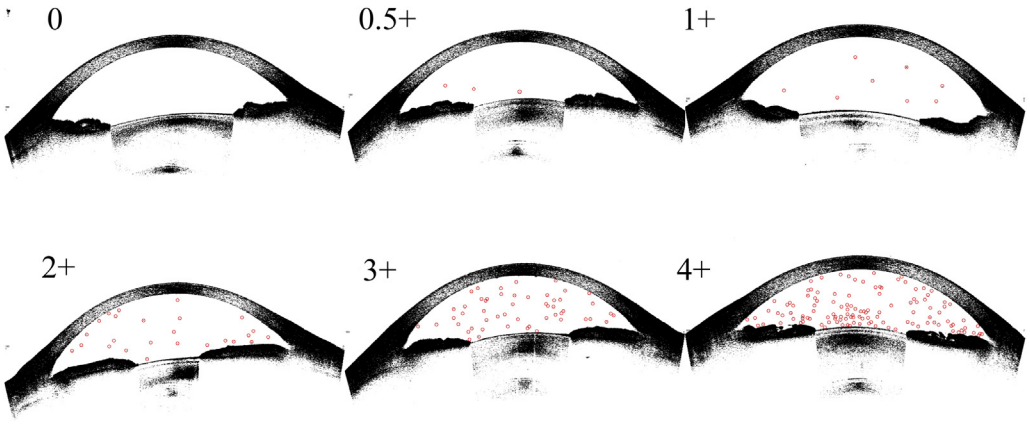

FIGURE 1. Hyperreflective dots in the aqueous humor. Representative anterior segment optical coherence tomography images of eyes from each uveitis severity level (0-4+) subgroup showing the association of inflammation severity with anterior chamber cell number. All images were acquired in the horizontal orientation (0°-180°) and binarized. Hyperreflective dots in the aqueous humor are thought to represent anterior chamber cells. The counted hyperreflective dots are marked by red circles. Hyperreflective dot number in the aqueous humor increased with clinical grade.

used for all statistical analyses. Normality of all datasets was assessed using the Shapiro-Wilk test ($P = 0.1$) and homogeneity of variance using the Levene test ($P = 0.1$). Normally distributed continuous variables are expressed as $\bar{x} \pm s$ while nonparametric datasets are expressed as median and interquartile range (IQR). The χ^2 test was used to compare sex ratio and the nonparametric Kruskal-Wallis test was used to compare differences in BCVA, PCSS-MAX, PCSS-MIN, PCSS-AVG, number of cells on OCT, and ARI index among active uveitis, inactive uveitis, and control groups. The Mann-Whitney *U* test was performed to compare 2 groups, followed by Bonferroni test to make a correction for further comparisons. Associations between hyperreflective dot number and SUN cell grade and between ARI index and clinical SUN flare grade were assessed using Spearman correlation analysis. We constructed receiver operating characteristic (ROC) curves of PCSS-MIN, PCSS-MAX, and PCSS-AVG to define the best indicator for KP diagnosis. We also constructed ROC curves of ARI index, hyperreflective dot number, and PCSS-MAX for total uveitis and active uveitis groups to analyze the utility of these metric for diagnosis and to calculate the Younden index. All tests were 2-tailed with a significance value of 0.05 (except for the Shapiro-Wilk and Levene tests). In addition, repeatability and reproducibility of hyperreflective dot count and ARI Index were assessed using the intraclass correlation coefficient, coefficient of variation, paired *t* tests and a Bland-Altman analysis.

RESULTS

• **PATIENT DEMOGRAPHICS AND CLINICAL CHARACTERISTICS:** Ninety-one eyes of 62 patients with uveitis involving the AS (either anterior uveitis or panuveitis) and 48 control eyes of 24 healthy individuals were included in this study. All patients had no presence of visible hypopyon observed by slit lamp. The demographic and clinical features of all participants are summarized in Table 1. Age and central corneal thickness (CCT) distribution were relatively consistent among groups. The proportion of females was significantly higher in the active inflammation group than in control and inactive uveitis groups. As expected, median BCVA was significantly higher in the control group than in either the active or inactive uveitis group ($P < 0.001$), but no significant differences were found between inactive and active groups ($P = 1.00$).

• **QUANTITATIVE ANALYSIS OF AC CELLS:** AC inflammation was graded from 0-4 according to the SUN criteria. Hyperreflective dot count (indicative of AC cell count) was significantly higher in the active uveitis group than the inactive uveitis and control groups (both $P < 0.001$; Figure 3, A), while there was no significant difference between the inactive uveitis and control groups ($P = 1.0$). We also assessed the correlation between SUN classification and hyperreflective dot count across the entire cohort. Eyes of all participants were divided into 6 categories according to SUN grade (0, 0.5+, 1+, 2+, 3+, and 4+). The median number and interquartile range of hyperreflective dots for each category are summarized in Table 2. The number of hyperreflective dots on OCT was positively correlated with SUN clinical grade ($r_s = 0.98$; $P < 0.001$; Figure 4, A). The hyperreflective dot count demonstrated good repeatability and reproducibility in the Supplemental Material.

• **QUANTITATIVE ANALYSIS OF AQUEOUS FLARE:** We used the ARI index to quantify AC flare according to a

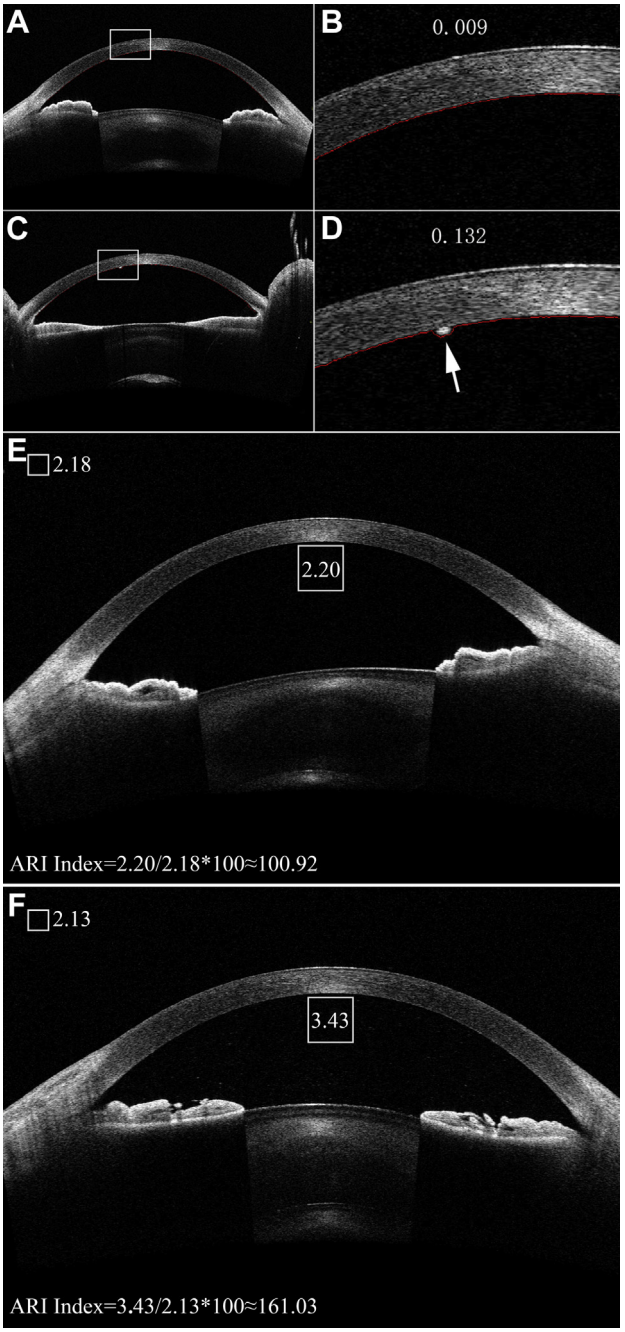

FIGURE 2. The posterior corneal surface smoothness and the anterior segment for aqueous-to-air relative intensity index. Assessment of corneal smoothness as a metric for keratic precipitates. (A) The posterior corneal surface of the control group was smooth. (B) Enlarged image of the area defined by the white box in (A). The posterior corneal surface smoothness value as calculated by our dedicated program was 0.009. (C) The posterior corneal surface of a cornea with KPs is not smooth. (D) Enlarged image of the area defined by the white box in (C) showing a KP (white arrow). The posterior corneal surface smoothness value calculated by the program was 0.132. Swept-source optical coherence tomography of the anterior segment for aqueous-to-air relative intensity index calculation in 2 different participants. The selected area is indicated by a white square. The number represents the average brightness of the area. The calculation formula is shown. (E) In this control participant, the aqueous-to-air relative intensity index score was 100.92. (F) In this patient with active uveitis, the aqueous-to-air relative intensity index score was 161.03.

previous study.[17] We selected 8 scan images per eye to allow for more objective results. The ARI index was significantly higher in the active uveitis group than the inactive uveitis and control groups ($P < 0.001$, Figure 3, B). Eyes from all participants were divided according to SUN flare grade into 5 categories (0, 1+, 2+, 3+, and 4+).[6] The IQR for each category, median ARI index on OCT, and the number of eyes are summarized in Table 3. The ARI index was positively correlated with SUN flare grade ($r_s = 0.79$; $P < 0.001$; Figure 4, B). The ARI index demonstrated good repeatability and reproducibility in the Supplemental Material.

• **QUANTITATIVE ANALYSIS OF KPS:** The PCSS values (maximum, minimum, and average) of 128 scan images from each eye were calculated automatically. PCSS-MAX, which represents the smoothness of the entire posterior corneal surface, differed significantly among groups ($P < 0.001$; Figure 5, A). PCSS-AVG, which represents the smoothness of the entire posterior corneal surface, was significantly higher in the active group than in the inactive and control groups ($P < 0.001$; Figure 5, B) and was also significantly higher in the inactive than control group ($P = 0.007$; Figure 5, B). Finally, PCSS-MIN, which represents the smoothness of the entire posterior corneal surface, was also significantly higher in active uveitis patients than in inactive patients and controls ($P = 0.003$ and $P = 0.002$, respectively; Figure 5, C), while there was no significant difference between the control and inactive groups ($P = 1.000$; Figure 5, C). To identify the best indicator for diagnosing KPs, we constructed individual ROC curves (Table 4). The area under the curve (AUC) for PCSS-MAX was larger than those for PCSS-AVG and PCSS-MIN (Figure 6, A), suggesting that PCSS-MAX is the best indicator for diagnosing KPs.

• **ROC CURVE ANALYSIS FOR UVEITIS DIAGNOSIS:** We also constructed ROC curves to assess the utilities of PCSS-MAX, hyperreflective dot number, and ARI index for diagnosing uveitis in general (both active and inactive) (Table 4), Again, the AUC for PCSS-MAX was larger than those for hyperreflective dots and ARI index (Figure 6, B), suggesting that PCSS-MAX is also the best indicator for diagnosing general uveitis. However, the AUC for active uveitis diagnosis was larger for hyperreflective dots than for PCSS-MAX and ARI index, indicating that the hyperreflective dot count is the best indicator for diagnosing active uveitis among patients with uveitis (Figure 6, C).

TABLE 1. Demographic and Clinical Features of Patient and Control Groups

Feature	Controls (n = 48)	Inactive Uveitis (n =35)	Active Uveitis (n = 56)	*P* Value[a]	Controls vs Inactive Uveitis[b]	Controls vs Active Uveitis[b]	Inactive Uveitis vs Active Uveitis[b]
Age (y)	36 ± 15	40 ± 16	40 ± 15	.226	—	—	—
Sex (male:female)	1:0.9	1:0.9	1:1.3	.584[c]	—	—	—
BCVA (decimal)	0.90 (0.8-1.0)	0.5 (0.4-0.6)	0.5 (0.3-0.6)	<.001	<.001	<.001	1.00
Max PCSS	0.091 (0.081-0.098)	0.169 (0.096-0.237)	0.212 (0.158-0.288)	<.001	<.001	<.001	<.001
Min PCSS	0.003 (0.001-0.005)	0.002 (0.001-0.005)	0.009 (0.002-0.028)	<.001	1.00	.003	.002
AVG PCSS	0.038 (0.029-0.047)	0.057 (0.039-0.077)	0.085 (0.061-0.114)	<.001	.007	<.001	<.001
ARI index	96.990 (91.74-100.00)	103.35 (98.16-106.76)	116.87 (109.58-127.68)	<.001	.023	<.001	<.001
No. of hyperreflective dots	0-0	0-0	4-25	<.001	1.00	<.001	<.001
CCT (mm)	544.9 ± 45.1	547.8 ± 72.6	545.8 ± 47.6	.819	—	—	—

ARI = aqueous-to-air relative intensity; BCVA = best-corrected visual acuity; CCT = central corneal thickness; OCT = optical coherence tomography; PCSS = posterior corneal surface smoothness.

Age and CCT are expressed as mean ± standard deviation, while BCVA, PCSS, ARI index, and number of cells on OCT are expressed as median (interquartile range).

[a]Compared with all other groups (Kruskal-Wallis test).

[b]Compared with 1 other group by Mann-Whitney *U* test with Bonferroni correction for multiple comparison.

[c]χ^2 test.

DISCUSSION

UVEITIS IS AMONG THE MOST SERIOUS SIGHT-threatening ophthalmic diseases, and afflicts tens of thousands of individuals across the globe.[1–4] The accurate evaluation of intraocular inflammation is crucial for monitoring uveitis severity, guiding treatment decisions, and assessing treatment efficacy.[1] Currently, AC inflammation is graded subjectively from slit lamp images based on the SUN criteria, so accuracy depends on the experience of the operator.[7] Therefore, objective methods and quantitative scales are needed to estimate the severity of uveitis activity, disease progression, and treatment response with greater accuracy and consistency.

AC cell counting is currently the predominant parameter used to diagnose uveitis and evaluate medication response. The number of AC cells, which appear as moving dust-like particles on slit lamp images, is strongly associated with the severity of inflammation in uveitis.[27] On AS-OCT images, AC cells appear as hyperreflective dots.[12–18] However, the major limitation of previous AS-OCT technologies is that they could not cover the whole AC. Moreover, some OCT instruments are insufficiently sensitive to detect cells in the deeper AC. Also, counting mainly depends on a single scan or even 1 OCT single-scan image.

Unlike previous devices, the CASIA2 instrument 1) uses a longer wavelength (1310 nm) to image deeper regions of the AC, 2) has superior resolution (axial resolution <10 μm, lateral resolution <30 μm) which can effectively detect inflammatory cells as small as 10-20 μm, and 3) can provide pseudo–3-dimensional imaging of the entire AC using the GLOBAL scan mode.[28] We therefore evaluated AC inflammation in uveitis involving the AS using this instrument. First, we measured inflammation severity over the entire AC using the AS GLOBAL SCAN mode. Currently, there is no specific protocol to guide OCT technicians in imaging the AC at specific locations, such as 45°, 90°, 135°, and 180°. The distribution of aqueous humor cells is influenced mainly by local circulation, and the specific points of imaging differ among examinations, which contributes to statistical variation and inconsistencies in counting hyperreflective dots.[16] We compensated for this variability by calculating the average number of hyperreflective dots in 8 OCT scan images. Consistent with previous studies,[12–15,17,18,29] hyperreflective dot number differed significantly between active and inactive uveitis, and was positively correlated with SUN cell grade, indicating that this count can be used for objective grading of AC cell number as a measure of inflammation severity. Furthermore, ROC curve analysis showed that the AUC of hyperreflective dots was larger than that of the ARI index or PCSS-MAX for diagnosing active uveitis. These results have also been verified in clinical practice. Thus, as a measure of AC cell number, hyperreflective dot count is a

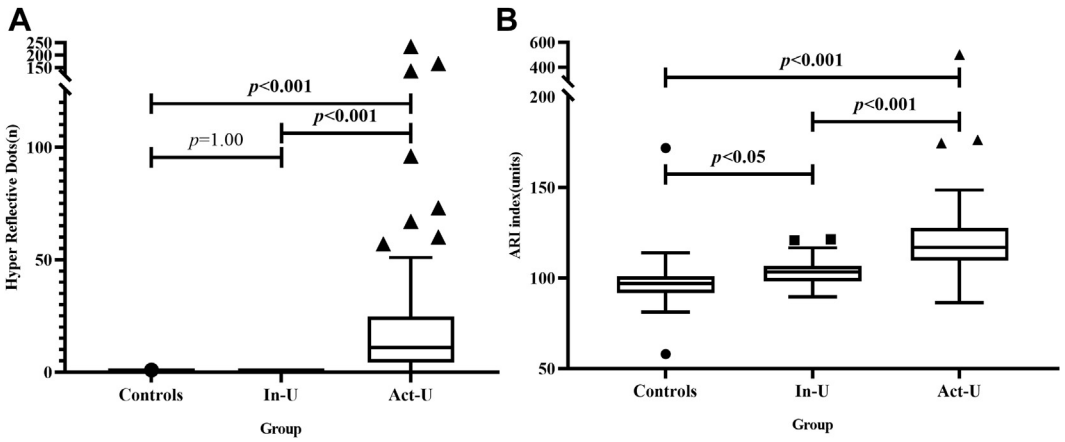

FIGURE 3. Hyperreflective dots and aqueous-to-air relative intensity (ARI) index in patients with uveitis and control subjects. The average number of hyperreflective dots in the anterior chamber and ARI were set as parameters for diagnosis. (A) The box plot shows the average number of hyperreflective dots and the ARI index for all participants. There was no significant difference in mean hyperreflective dot count between the control and inactive uveitis groups ($P = 1.00$). However, the mean hyperreflective dot count was significantly higher in patients with active uveitis than control subjects and patients with inactive uveitis ($P < 0.001$). (B) The ARI index differed significantly between patients with inactive uveitis and control subjects ($P < 0.05$), and was also significantly higher in patients with active uveitis than in patients with inactive uveitis ($P < 0.001$).

TABLE 2. Distribution of the Mean Hyperreflective Dot Number on Optical Coherence Tomography According to Standardization of Uveitis Nomenclature Clinical Grade

Clinical Grade	Eyes (n)	Hyperreflective Dots
0	83	0 (0-0)
0.5+	8	3 (2-4)
1+	18	5 (3-7)
2+	21	20 (13-24)
3+	6	58 (49-69)
4+	3	151 (106-207)

All values expressed as median (interquartile range).

promising indicator for uveitis prognosis and treatment guidance.

To achieve an objective and comprehensive assessment of AC inflammation, we investigated additional AS-OCT–derived indicators, including aqueous flare and KPs. Aqueous flare refers to the flashing lights and floating particles observed under slit lamp after inflammatory exudate enters the aqueous humor. AC flare has been demonstrated as an indicator of AC inflammation.[6] Similarly, the ARI index can be used to assess AC inflammation.[17] However, the value is highly dependent on the measurement area selected. In the current study, we averaged multiple scans to calculate this index and found that ARI index differed significantly between active and inactive uveitis groups and was strongly associated to SUN flare grade. However, ARI index also differed significantly between the control and inactive uveitis group, inconsistent with previous studies.[17] This discrepancy may be explained by the effects of corneal absorption and reflection on the OCT signal and the documented associations between ARI index and factors, such as patient age and BCVA.[17] Furthermore, the calculation of ARI index replies on signal strength inside and outside the eye, which could be confounded by lighting and corneal conditions, such as corneal haze, edema and even tear film stability. At present, there are few studies on ARI index. Nonetheless, our findings suggest that ARI index is a promising indicator for quantifying AC flare.

KPs are formed from inflammatory cells by convection within the aqueous humor and deposition on the posterior corneal surface. Although KPs cannot be used to estimate inflammatory activity in uveitis, they are important signs of anterior uveitis.[29] KPs can be detected by AS-OCT and appear as hyperreflective masses on the posterior aspect of the cornea.[30] The main advantage of CAISA2 for KP detection is the pseudo–3-dimensional scan mode, which uses 128 scans to cover almost the entire cornea. We designed an algorithm to quantify the degree of PCSS from all 128 OCT images from each eye and calculated the maximum, minimum, and average values. Nonparametric testing and ROC curve analysis indicated that PCSS-MAX is a better indicator for the diagnosis of KPs than PCSS-AVG. This differential efficacy is likely because of the variation in KP distribution. ROC curve analysis also revealed that PCSS-MAX was suitable for diagnosis of uveitis in general (both active and inactive). This capacity for distinguishing uveitis compensates for the inability of hyperreflective dot count to distinguish healthy eyes from inactive uveitis. Dynamic changes in

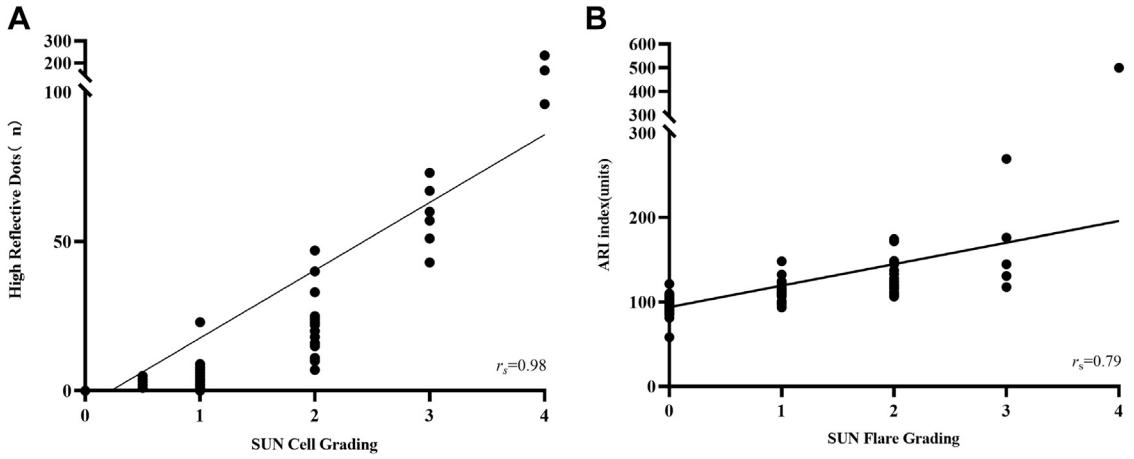

FIGURE 4. Correlations between Standardization of Uveitis Nomenclature (SUN) grade and both hyperreflective dot number and aqueous-to-air relative intensity (ARI) index. Correlational analysis of optical coherence tomography parameters with SUN grades. Scatter plots show the correlation between hyperreflective dot count and clinical SUN cell grade and between the ARI index and clinical SUN flare grade. (A) Hyperreflective dot count increased significantly with SUN grade ($r_s = 0.98$, $P < 0.001$). (B) The corresponding ARI index also increased with SUN flare grade ($r_s = 0.79$, $P < 0.001$).

TABLE 3. Distribution of Mean Aqueous-to-Air Relative Index on Optical Coherence Tomography According to Standardization of Uveitis Nomenclature Clinical Grade

Clinical Flare Grade	Eyes (n)	ARI Index
0	83	99.53 (93.48-103.73)
1+	25	112.39 (107.79-116.86)
2+	25	121.82 (115.98-131.71)
3+	5	144.60 (124.16-222.80)
4+	1	500[a]

ARI = aqueous-to-air relative intensity.
All values expressed as median (interquartile range).
[a]Not calculated because of small sample size.

KPs can also be used to assess AC inflammation. For example, the disappearance of KPs may indicate an improvement in inflammation, while an increasing number of KPs suggests worsening of inflammation. Therefore, KPs are an essential indicator for clinicians even if they do not directly represent inflammatory activity. Our study provides an objective method to quantify KPs and demonstrates that PCSS-MAX can aid in the assessment of AC inflammation. Interestingly, when we counted 78 patients with the presence of KPs, we found that 63% of PCSS MAX occurred in the position 45°-225° to 135°-315°. This position corresponds to Arlt's triangle. This suggests that more robust information is hidden in Arlt's triangle. Based on this success, additional quantitative corneal algorithms warrant further exploration.

This study has several limitations. First, although most of the AC cells are white blood cells, this method of counting hyperreflective dots cannot distinguish among white blood cells, floating pigment, or other floaters. Second, ARI index analysis relies on manual selection of measurement area. Although we selected multiple scan images to calculate the mean, the manual selection of measurement area may still introduce subjective variability. Moreover, the algorithm in this research could not differentiate various forms of KPs and other endothelial deposits. In future research, we also need to further optimize our algorithm to achieve more accurate quantification of KPs and other confounding factors. Finally, larger-scale studies involving multiple centers are required to confirm the clinical utility of this quantitative AS-OCT–based method for uveitis diagnosis, severity grading, and treatment evaluation.

In conclusion, our study shows that the new AS-OCT system CASIA2 can be used to diagnose AC inflammation in uveitis by quantifying AC cell number, AC flare, and KPs.

CRediT AUTHORSHIP CONTRIBUTION STATEMENT

MINGZHI LU: SOFTWARE, WRITING - ORIGINAL DRAFT. **Xiaoran Wang:** METHODOLOGY, WRITING - ORIGINAL DRAFT. **LEI LEI:** METHODOLOGY, WRITING - ORIGINAL DRAFT, FUNDING ACQUISITION. **YANG DENG:** INVESTIGATION, WRITING - REVIEW & EDITING. **TINGLONG YANG:** FORMAL ANALYSIS, VISUALIZATION, DATA CURATION. **YE DAI:** RESOURCES, INVESTIGATION. **YONGHAO LI:** METHODOLOGY, RESOURCES. **XIAOLIANG GAN:** FUNDING ACQUISITION, RESOURCES. **YIXIN HU:** VALIDATION, INVESTIGATION. **HUI CHEN:** VALIDATION, INVESTIGATION.

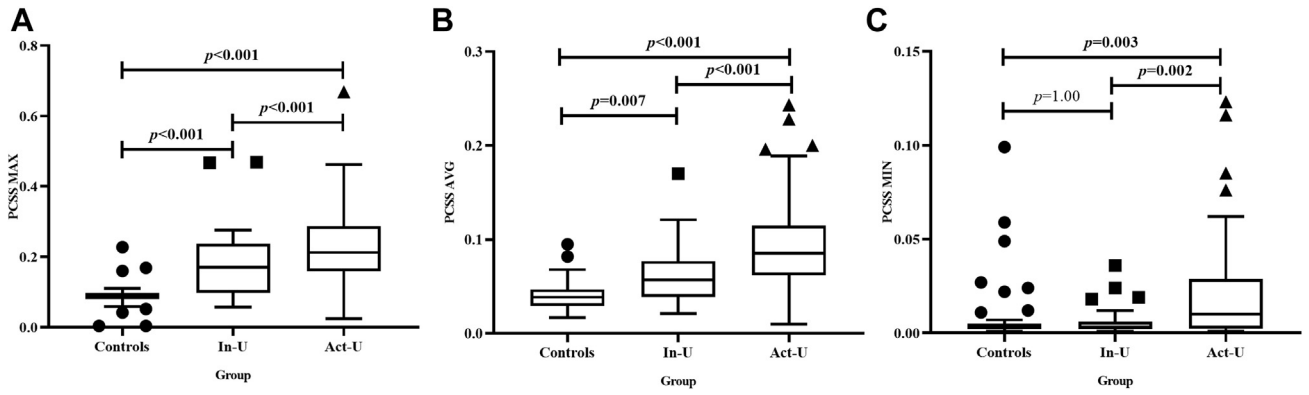

FIGURE 5. The maximum, minimum, and average posterior corneal surface smoothness (PCSS) values were calculated and compared. PCSS was taken as the parameter for diagnosis. Maximum, minimum, and average PCSS values were calculated from 128 scan images per eye to evaluate keratic precipitates (KPs). (A) PCSS-MAX differed significantly among groups ($P < 0.001$). (B) PCSS-AVG was significantly higher in the active group than the inactive and control groups ($P < 0.001$) and was also significantly higher in the inactive than control group ($P = 0.007$). (C) PCSS-MIN was also significantly higher in patients with active uveitis than patients with inactive uveitis and control subjects ($P = 0.003$ and $P = 0.002$, respectively), while there was no significant difference between control and inactive groups ($P = 1.00$).

TABLE 4. Receiver Operating Characteristic Curve Analysis

Item	Diagnosis	AUC (95% CI)	*P* Value (AUC)	Sensitivity (%)	Specificity (%)
PCSS-MAX	KPs	0.97 (0.92-0.99)	<.001	98.70	88.71
PCSS-AVG	KPs	0.94 (0.88-0.97)	<.001	90.91	82.23
PCSS-MIN	KPs	0.71 (0.66-0.78)	<.001	64.94	69.35
PCSS-MAX	Uveitis	0.89 (0.82-0.93)	<.001	82.42	81.25
ARI index	Uveitis	0.85 (0.78-0.90)	<.001	72.53	89.58
No. of hyperreflective dots	Uveitis	0.81 (0.73-0.87)	<.001	81.54	100
PCSS-MAX	Active uveitis	0.81 (0.74-0.88)	<.001	92.88	71.08
ARI index	Active uveitis	0.89 (0.83-0.94)	<.001	89.29	84.34
No. of high reflective dots	Active uveitis	0.98 (0.95-0.99)	<.001	98.21	98.80

ARI = aqueous-to-air relative intensity; AUC = area under the curve; CI = confidence interval; KP = keratic precipitates; PCSS = posterior corneal surface smoothness.

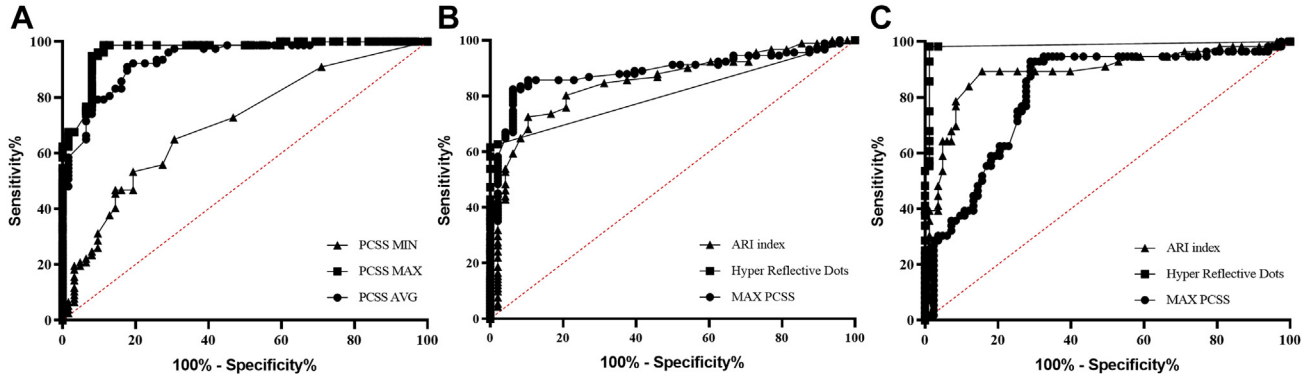

FIGURE 6. Receiver operating characteristic (ROC) curves were constructed to test the values of these indicators for uveitis diagnosis. ROC curve was analyzed to identify quantitative indicators for keratotic precipitates, uveitis, and active uveitis. (A) Posterior corneal surface smoothness maximum (PCSS-MAX) was the best indicator for diagnosing KPs according to the area under the curve (AUC = 0.97). (B) PCSS-MAX was also the best indicator for diagnosing uveitis (AUC = 0.89). (C) Hyperreflective dot count was the best indicator for diagnosing active uveitis (AUC = 0.99).

MENG LI: VALIDATION, VISUALIZATION. **LISHI SU:** INVESTIGATION. **JIN YUAN:** CONCEPTUALIZATION, METHODOLOGY, RESOURCES, WRITING - REVIEW & EDITING. **WEI CHI:** CONCEPTUALIZATION, METHODOLOGY, RESOURCES, WRITING - REVIEW & EDITING, FUNDING ACQUISITION, SUPERVISION, PROJECT ADMINISTRATION.

ALL AUTHORS HAVE COMPLETED AND SUBMITTED THE ICMJE FORM FOR DISCLOSURE OF POTENTIAL CONFLICTS OF INTEREST. Funding/Support: Supported by grants from the Science and Technology Project of Guangzhou (201804010415; Dr Chi), the National Natural Science Foundation of China (81571884; Dr Gan), and the Science and Technology Project of Guangzhou (2018A030313573; Dr Lei). Financial Disclosures: The authors indicate no financial conflict of interest. All authors attest that they meet the current ICMJE criteria for authorship.

Drs Lu, Wang, and Lei served jointly as first authors.

REFERENCES

1. Jabs DA. Epidemiology of uveitis. *Ophthalmic Epidemiol* 2008;15(5):283–284.
2. Durrani OM, Meads CA, Murray PI. Uveitis: a potentially blinding disease. *Ophthalmologica* 2004;218(4):223–236.
3. Williams GJ, Brannan S, Forrester JV, et al. The prevalence of sight-threatening uveitis in Scotland. *Br J Ophthalmol* 2007;91(1):33–36.
4. Rothova A, Suttorp-van Schulten MS, Frits Treffers W, Kijlstra A. Causes and frequency of blindness in patients with intraocular inflammatory disease. *Br J Ophthalmol* 1996;80(4):332–336.
5. Gutteridge IF, Hall AJ. Acute anterior uveitis in primary care. *Clin Exp Optom* 2007;90(2):70–82.
6. Jabs DA, Nussenblatt RB, Rosenbaum JT. Standardization of uveitis nomenclature for reporting clinical data. Results of the First International Workshop. *Am J Ophthalmol* 2005;140(3):509–516.
7. Wong IG, Nugent AK, Vargas-Martín F. The effect of biomicroscope illumination system on grading anterior chamber inflammation. *Am J Ophthalmol* 2009;148(4):516–520.e512.
8. Sawa M, Tsurimaki Y, Tsuru T, Shimizu H. New quantitative method to determine protein concentration and cell number in aqueous in vivo. *Jpn J Ophthalmol* 1988;32(2):132–142.
9. Tugal-Tutkun I, Herbort CP. Laser flare photometry: a noninvasive, objective, and quantitative method to measure intraocular inflammation. *Int Ophthalmol* 2010;30(5):453–464.
10. Yeo TH, Ilangovan S, Keane PA, Pavesio C, Agrawal R. Discrepancies in assessing anterior chamber activity among uveitis specialists. *Jpn J Ophthalmol* 2016;60(3):206–211.
11. Ladas JG, Wheeler NC, Morhun PJ, Rimmer SO, Holland GN. Laser flare-cell photometry: Methodology and clinical applications. *Surv Ophthalmol* 2005;50(1):27–47.
12. Agarwal A, Ashokkumar D, Jacob S, Agarwal A, Saravanan Y. High-speed optical coherence tomography for imaging anterior chamber inflammatory reaction in uveitis: clinical correlation and grading. *Am J Ophthalmol* 2009;147(3):413–416.e413.
13. Igbre AO, Rico MC, Garg SJ. High-speed optical coherence tomography as a reliable adjuvant tool to grade ocular anterior chamber inflammation. *Retina* 2014;34(3):504–508.
14. Sharma S, Lowder CY, Vasanji A, Baynes K, Kaiser PK, Srivastava SK. Automated analysis of anterior chamber inflammation by spectral-domain optical coherence tomography. *Ophthalmology* 2015;122(7):1464–1470.
15. Edmond M, Yuan A, Bell BA, et al. The feasibility of spectral-domain optical coherence tomography grading of anterior chamber inflammation in a rabbit model of anterior uveitis. *Invest Ophthalmol Vis Sci* 2016;57(9):OCT184–OCT188.
16. Li Y, Lowder C, Zhang X, Huang D. Anterior chamber cell grading by optical coherence tomography. *Invest Ophthalmol Vis Sci* 2013;54(1):258–265.
17. Invernizzi A, Marchi S, Aldigeri R, et al. Objective quantification of anterior chamber inflammation: Measuring cells and flare by anterior segment optical coherence tomography. *Ophthalmology* 2017;124(11):1670–1677.
18. Baghdasaryan E, Tepelus TC, Marion KM, et al. Analysis of ocular inflammation in anterior chamber-involving uveitis using swept-source anterior segment OCT. *Int Ophthalmol* 2019;39(8):1793–1801.
19. Choi WJ, Pepple KL, Wang RK. Automated three-dimensional cell counting method for grading uveitis of rodent eye in vivo with optical coherence tomography. *J Biophotonics* 2018;11(9):e201800140.
20. Shoji T, Kato N, Ishikawa S, et al. In vivo crystalline lens measurements with novel swept-source optical coherent tomography: an investigation on variability of measurement. *BMJ Open Ophthalmol* 2017;1(1):e000058.
21. Zheng X, Goto T, Shiraishi A, Nakaoka Y. New method to analyze sagittal images of upper eyelid obtained by anterior segment optical coherence tomography. *Orbit* 2019;38(6):446–452.
22. Xu BY, Penteado RC, Weinreb RN. Diurnal variation of optical coherence tomography measurements of static and dynamic anterior segment parameters. *J Glaucoma* 2018;27(1):16–21.
23. Kimura S, Morizane Y, Shiode Y, et al. Assessment of tilt and decentration of crystalline lens and intraocular lens relative to the corneal topographic axis using anterior segment optical coherence tomography. *PLoS One* 2017;12(9):e0184066.
24. Igarashi A, Shimizu K, Kato S, Kamiya K. Predictability of the vault after posterior chamber phakic intraocular lens implantation using anterior segment optical coherence tomography. *J Cataract Refract Surg* 2019;45(8):1099–1104.
25. Satou T, Kato S, Igarashi A, et al. Prediction of pupil size under binocular open-view settings using the new CASIA2 device. *Int Ophthalmol* 2019;39(4):791–796.
26. Xu BY, Mai DD, Penteado RC, Saunders L, Weinreb RN. Reproducibility and agreement of anterior segment parameter measurements obtained using the CASIA2 and spectralis OCT2 optical coherence tomography devices. *J Glaucoma* 2017;26(11):974–979.

27. Krishna U, Ajanaku D, Denniston AK, Gkika T. Uveitis: a sight-threatening disease which can impact all systems. *Postgrad Med J* 2017;93(1106):766–773.
28. Prinyakupt J, Pluempitiwiriyawej C. Segmentation of white blood cells and comparison of cell morphology by linear and naïve Bayes classifiers. *Biomed Eng Online* 2015;14(1):63.
29. Agrawal RV, Murthy S, Sangwan V, Biswas J. Current approach in diagnosis and management of anterior uveitis. *Indian J Ophthalmol* 2010;58(1):11–19.
30. Hixson A, Blanc S, Sowka J. Monitoring keratitis resolution with optical coherence tomography. *Optom Vis Sci* 2014;91(4 suppl 1):S40–S45.